# The resistive transition and Meissner effect in carbon nanotubes: Evidence for quasi-one-dimensional superconductivity above room temperature

Guo-meng Zhao*

*Department of Physics and Astronomy, California State University at Los Angeles, Los Angeles, CA 90032, USA*

It is well known that copper-based perovskite oxides rightly enjoy consensus as high-temperature superconductors on the basis of two signatures: the resistive transition and the Meissner effect. We show that the resistive transitions in carbon nanotubes agree quantitatively with the Langer-Ambegaokar-McCumber-Halperin (LAMH) theory for quasi-1D superconductors although the superconducting transition temperatures can vary from 0.4 K to 750 K for different samples. We have also identified the Meissner effect in the field parallel to the tube axis up to room temperature for aligned and physically separated multi-walled nanotubes (MWNTs). The magnitude of the Meissner effect is in quantitative agreement with the predicted penetration depth from the measured carrier density. Furthermore, the bundling of individual MWNTs into closely packed bundles leads to a large enhancement in the diamagnetic susceptibility, which is the hallmark of the Josephson coupling among the tubes in bundles. These results consistently indicate quasi-1D high-temperature superconductivity in carbon nanotubes.

## I. INTRODUCTION

It is well known that copper-based perovskite oxides rightly enjoy consensus as high-temperature superconductors on the basis of two signatures: the Meissner effect and the sharp resistive transition to the zero resistance state. In contrast, these two important signatures are far less obvious in a quasi-one-dimensional (quasi-1D) superconducting wire that has a finite number of transverse conduction channels and a very thin transverse dimension. Due to large superconducting fluctuations, the resistive transition in quasi-1D superconductors could be very broad. Because of the finite number of transverse channels, the four-probe resistance never goes to zero even though the on-wire resistance approaches zero. Because the penetration depth is far larger than the transverse dimension, the Meissner effect becomes very small and less visible. These unique features make it difficult to unambiguously identify quasi-1D superconductivity in altrathin wires or tubes.

Previously we have provided over twenty pieces of evidence (see two review articles[1,2] and references therein) for quasi-1D high-temperature superconductivity in individual single-walled carbon nanotubes (SWNTs), in SWNT bundles/mats, in individual multi-walled nanotubes (MWNTs), and in MWNT mats. Here we make quantitative data analyses on the observed resistive transitions and magnetic properties in carbon nanotubes. We find that the resistive transitions in carbon nanotubes agree quantitatively with the Langer-Ambegaokar-McCumber-Halperin (LAMH) theory[3] for quasi-1D superconductors although the superconducting transition temperatures vary from 0.4 K to 750 K for different samples. We have also identified the Meissner effect in the field parallel to the tube axis up to room temperature for aligned MWNTs that are physically separated. The magnitude of the Meissner effect is in quantitative agreement with the predicted penetration depth from the measured carrier density. Furthermore, the diamagnetic susceptibility in closely packed MWNT bundles increases by a factor of over 4 at low temperatures compared with that for physically separated tubes. This is the hallmark of the Josephson coupling among the tubes in bundles. These results consistently indicate quasi-1D high-temperature superconductivity in carbon nanotubes.

## II. THEORETICAL DESCRIPTION FOR THE RESISTIVE TRANSITION IN QUASI-1D SUPERCONDUCTORS

The phenomenon of superconductivity depends on the coherence of the phase of the superconducting order parameter. The phase coherence of the superconducting order parameter leads to the zero-resistance state. For three-dimensional (3D) bulk systems, the transition to the zero-resistance state occurs right below the mean-field superconducting transition temperature $T_{c0}$ such that the resistive transition is very sharp and the transition width is negligibly small. In contrast, the resistive transition in quasi-1D superconductors is broad because of large superconducting fluctuations. A quantum theory to describe the resistive transition in quasi-1D superconductors was developed by Langer, Ambegaokar, McCumber and Halperin (LAMH)[3] over 30 years ago. The theory is based on thermally activated phase slips (TAPS), which cause the resistance to decrease to zero exponentially. In addition to the thermally activated phase slips, there are also quantum phase slips due to a finite number of transverse channels[4], which prevent altrathin wires or tubes from being true superconductors with absolutely zero resistance.

Very recently, we have shown[5] that the observed re-

sistive transition of a superconducting carbon nanotube bundle ($T_{c0} = 0.44$ K ) is in quantitative agreement with the LAMH theory. We have also demonstrated that[5] the resistive transition below $T_c^* = 0.90T_{c0}$ is simply proportional to $\exp(-\frac{3\beta T_c^*}{T}(1-\frac{T}{T_c^*})^{3/2})$, where the barrier height has the same form as that predicted by the LAMH theory. The quantitative agreement between theory and experiment indicates that the LAMH theory can correctly describe the resistive transition in the low-$T_c$ superconducting carbon nanotube bundle. Then, a natural way to demonstrate high-temperature superconductivity in other carbon nanotubes is to see whether the observed resistive transitions agree with the LAMH theory in a quantitative way.

For two-probe or four-probe measurements on carbon nanotubes with finite transverse channels, the total resistance is $R = R_0 + R_{tube}$, where $R_{tube}$ is the on-tube resistance and $R_0 = R_t = R_Q/tN_{ch}$ for four-probe measurements, or $R_0 = R_Q/tN_{ch} + R_c$ for two probe measurements[6]. Here $t$ is the transmission coefficient ($t \leq 1$), $R_Q = h/2e^2 = 12.9$ k$\Omega$ is the resistance quantum, $R_c$ is the contact resistance, and $R_t$ is the tunneling resistance. Both $R_c$ and $R_t$ should be temperature independent. For ideal contacts, $R_c = 0$ and $t = 1$, so $R_0 = R_t = 12.9$ k$\Omega/N_{ch}$ for a bundle comprising $N_{ch}$ transverse channels. For quasi-1D systems, $N_{ch}$ is always finite such that both four-probe and two-probe resistances never go to zero even if the on-tube resistance is zero. Only if $N_{ch}$ goes to infinity, as in the bulk 3D systems, $R_t$ becomes zero such that four probe resistance can go to zero below the superconducting transition temperature. Therefore, the non-zero four-probe resistance in altrathin tubes does not rule out superconductivity in the tubes.

According to the LAMH theory, the on-tube resistance is given by[5]

$$R_{tube} = \frac{m}{T^{1.5}}(1 - \frac{T}{T_{c0}})^{9/4} \exp[-\frac{3cT_{c0}}{T}(1 - \frac{T}{T_{c0}})^{3/2}], \quad (1)$$

with

$$m = 2.55T_{c0}(3cT_{c0})^{1/2}[\frac{L}{\xi(0)}], \quad (2)$$

and

$$c = 0.34N_{ch}\frac{\xi(0)}{\xi_{BCS}}. \quad (3)$$

Here $m$ is in the unit of k$\Omega$K$^{3/2}$, $\xi_{BCS}$ is the BCS coherence length, and $\xi(0)$ is the zero-temperature coherence length. In the clean limit, $\xi(0) = 0.74\xi_{BCS}$ and thus $c = 0.25N_{ch}$. The estimated region of validity for Eq. 1 is below $0.07R_N$ ($R_N$ is the normal-state resistance) for dirty wires where the mean free path $l << \xi_{BCS}$ (Ref.[7]). For cleaner wires, the region of validity increases. For example, the estimated regions of validity are below about $0.17R_N$ and $0.55R_N$ for $l = \xi_{BCS}$ and $l = 10\xi_{BCS}$, respectively. Moreover, we have found that[5] the on-tube

resistance below $T_c^* \simeq 0.9T_{c0}$ can be excellently described by

$$R_{tube} = \alpha \exp[-\frac{3\beta T_c^*}{T}(1 - \frac{T}{T_c^*})^{3/2}]. \quad (4)$$

Here the $\beta$ value is nearly the same as the $c$ value[5]. The microscopic origin of this simple empirical formula is unknown at present. In the following, we will compare these formulas with the measured resistive transitions in several different samples with $T_{c0}$'s ranging from 0.4 K to 750 K.

## III. THE RESISTIVE TRANSITION IN A SWNT BUNDLE WITH $T_{C0} = 0.44$ K

In 2001, Kociak *et al.* provided the first experimental evidence for superconductivity in single-walled carbon nanotube bundles from the electrical transport measurements[8]. Although the superconducting transition temperature is low ($< 1$ K), the resistive behavior of the nanotube bundle can serve as a prototype for the resistive transition in quasi-1D superconducting wires with a finite number of transverse conduction channels.
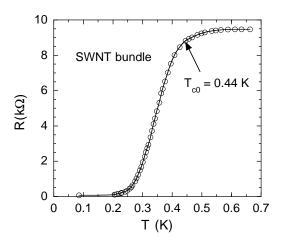


FIG. 1. The temperature dependence of the two-probe resistance for a SWNT bundle that consists of about 350 tubes. The data are extracted from Ref.[8].

Fig. 1 shows the two-probe resistance data for a SWNT bundle that consists of about 350 tubes[8]. One can see that the resistance starts to drop below about 0.5 K, decreases more rapidly below $T_{c0} \simeq 0.44$ K and saturates to a value of 74 $\Omega$. From the saturated value of $R_0 = 74$ $\Omega$, and the relation: $R_0 = R_Q/tN_{ch} + R_c$, one can easily find that more than 174 transverse channels are connected to the electrodes and participate in electrical transport. This implies that more than 87 metallic-chirality superconducting SWNTs take part in electrical transport. Considering the fact that one third of tubes should have metallic chiralities and become superconducting, we find the total number ($N_m$) of the superconducting tubes to be 117, implying that $t \geq 0.74$. The

value of $N_m$ can be also deduced from the measured current $I_c^*$ at which the last resistance jump occurs. The $I_c^*$ corresponds to the critical current for a superconducting wire without disorder and with the same number of the transverse channels[8]. For metallic chirality superconducting carbon nanotubes, one can readily deduce that[9] $I_c^* = 7.04 k_B T_{c0} N_m / e R_Q$. With $I_c^* = 2.4$ $\mu$A (Ref.[8]) and $T_{c0} = 0.44$ K, we have $N_m = 116$, in remarkably good agreement with the value deduced above.

In Fig. 2, we fit the resistance data below $0.88 T_{c0}$ by

$$R = R_0 + \alpha \exp[-\frac{3\beta T_c^*}{T}(1 - \frac{T}{T_c^*})^{3/2}]. \tag{5}$$

Here the first term is the sum of the tunneling and contact resistances and equal to 74 $\Omega$, and the second term is the on-tube resistance (see Eq. 4). We can see that the fit is excellent with the fitting parameters $\beta = 2.99 \pm 0.05$ and $T_c^* = 0.394 \pm 0.002$ K. Reducing or increasing the temperature region for the fit tends to worsen the fit quality. Therefore, the on-tube resistance goes to zero exponentially below $T_c^* = 0.9 T_{c0}$. In fact, the on-tube resistance may never go to zero if we consider quantum phase slips due to the finite number of transverse channels. Nevertheless, the on-tube resistance well below $T_{c0}$ should be negligibly small if $N_{ch}$ is not so small.
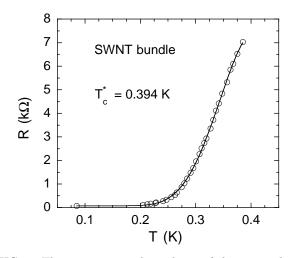
FIG. 2. The temperature dependence of the two-probe resistance for a SWNT bundle below $0.88 T_{c0}$. The solid line is the curve best fitted by Eq. 5 with $\beta = 2.99 \pm 0.05$ and $T_c^* = 0.394 \pm 0.002$ K. Reducing or increasing the temperature region for the fit tends to worsen the fit quality. It is striking that the on-tube resistance below $0.88 T_{c0}$ decreases exponentially to zero.

In Fig. 3, we fit the resistance data below $0.06 R_N$ by the following equation.

$$R = 74 + \frac{m}{T^{1.5}}(1 - \frac{T}{T_{c0}})^{9/4} \exp[-\frac{3c T_{c0}}{T}(1 - \frac{T}{T_{c0}})^{3/2}]. \tag{6}$$

Here the second term is the on-tube resistance which is the same as Eq. 1 predicted by the LAMH theory. We fit

the resistance data in this temperature region because $l << \xi_{BCS}$ is well satisfied in this SWNT bundle, as seen below. One can see that the fitting is very good with the fitting parameters: $m = 26.6 \pm 4.7$ k$\Omega K^{1.5}$ and $c = 3.08 \pm 0.13$. It is remarkable that the value of $c$ is nearly the same as the value of $\beta$ ($2.99 \pm 0.05$) deduced above from a simple exponential fit (Eq. 5).
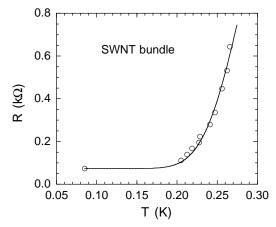
FIG. 3. The temperature dependence of the two-probe resistance for a SWNT bundle below $0.06 R_N$. The solid line is the curve fitted to the data below $0.06 R_N$ by Eq. 6 predicted by the LAMH theory. The estimated region of validity for the LAMH theory is below $0.07 R_N$ for dirty wires where $l << \xi_{BCS}$ (Ref.[7]). The condition of $l << \xi_{BCS}$ is well satisfied in the SWNT bundle (see text).

From the fitting parameters $c$ and $m$, and the measured normal-state resistance, we have deduced[5] $l = 46$ Å, $\xi(0) = 850$ Å, and $\xi_{BCS} = 21739$ Å. Using these values, we can calculate $c = 3.11$ from Eq. 3 and the critical current[5] $I_c = 62.4$ nA at 0.1 K. The calculated value of $c$ is nearly the same as that (3.08) deduced from the fitting, and the calculated value of $I_c$ is in quantitative agreement with the measured value (62 nA) at 0.1 K (Ref.[8]). Moreover, we can estimate the Fermi velocity $v_F$ from the deduced value of $\xi_{BCS}$ and the formula $\xi_{BCS} = 0.18 \hbar v_F / k_B T_{c0}$. With $\xi_{BCS} = 21739$ Å and $T_{c0} = 0.44$ K, we get $\hbar v_F = 4.6$ eVÅ. Then we estimate $\gamma_\circ = 2.16$ eV from the formula $\hbar v_F = 1.5 a_{C-C} \gamma_\circ$ (Ref.[10]). This value is very close to the value (2.4 eV) estimated from the first-principle calculation[11]. Thus, the resistance data of the SWNT bundle agrees with the LAMH theory in a quantitative way.

## IV. THE RESISTIVE TRANSITION IN A SINGLE MWNT WITH $T_{C0} = 262$ K

In 1996, Ebbesen *et al.* made the first four-probe resistance measurements on individual multi-walled carbon nanotubes[12]. Four 80-nm-wide tungsten leads were patterned by ion-induced deposition of tungsten from $W(CO)_6$ carrier gas. This technique makes it possible

for electrodes to connect multi-shells of the tubes[13]. It is interesting that the electrical properties vary significantly from samples to samples. Some tubes show abrupt jumps in resistivity when the temperature increases. In some other tubes, the resistance at room temperature is very small (e.g., 200 Ω) but a metal-insulator transition occurs below about 200 K. We will show that the resistive behavior in the former case is in quantitative agreement with that expected for quasi-1D superconductivity. The resistive behavior in the latter case may be explained by a superconductor-to-insulator transition in dirty quasi-1D systems.
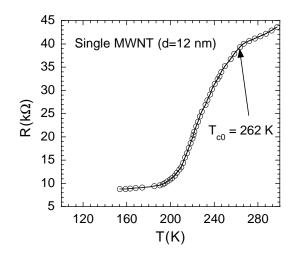


FIG. 4. The temperature dependence of the resistance for a single MWNT with $d \simeq 12$ nm. The data are extracted from Ref.[12].

Fig. 4 shows the four-probe resistance data for a single MWNT with a diameter of 12±2 nm. The inner contact distance is $L = 5000$ Å. One can see that the resistance drops more rapidly below about 262 K and saturates to a value of about 8.80 kΩ below 160 K. The resistive behavior of this single tube is similar to the resistive transition for a quasi-1D superconductor with $T_{c0} \simeq 262$ K. The finite resistance far below the superconducting transition temperature is due to a finite number of transverse channels, which is estimated to be about 54 for this tube (see below). Using $R_0 = 8.80$ kΩ, $N_{ch} = 54$, and the relation: $R_0 = R_Q/tN_{ch}$, we estimate the average $t$ for each channel to be about 0.013. The small value of $t$ suggests that the electrical contacts to the tube are rather poor. Assuming a negligible on-tube resistance below 160 K, we estimate that the on-tube resistance in the normal state (at 300 K) is about 34 kΩ, leading to $R_N/L = 68$ kΩ/$\mu$m.

In Fig. 5 we fit the resistance data below $T = 233$ K $= 0.89T_{c0}$ by Eq. 5 with a fixed $R_0 = 8.80$ kΩ. One can see that the fitting is excellent with the fitting parameters: $\beta = 11.71\pm0.12$, $\alpha = 19.0\pm0.1$ kΩ, and $T_c^* = 234$ K. It is interesting that $T_c^* = 0.89T_{c0}$, the same as that for the SWNT bundle with $T_{c0} = 0.44$ K.
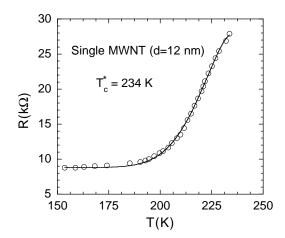


FIG. 5. The temperature dependence of the resistance for the 12-nm MWNT below 233 K $= 0.89T_{c0}$. The solid line is the curve best fitted by Eq. 5 with the fitting parameters: $\beta = 11.71\pm0.12$, $\alpha = 19.0\pm0.1$ kΩ, and $T_c^* = 234$ K, and with a fixed $R_0 = 8.80$ kΩ. Reducing or increasing the temperature region for the fit tends to worsen the fit quality.

In Fig. 6 we fit the resistance data below about $0.15R_N$ by

$$R = 8.80 + \frac{m}{T^{1.5}}(1 - \frac{T}{T_{c0}})^{9/4} \exp[-\frac{3cT_{c0}}{T}(1 - \frac{T}{T_{c0}})^{3/2}].$$ (7)

We fit the resistance data in this region because $l \simeq \xi_{BCS}$, as seen below. We can see that the fitting is excellent between 190 K and 210 K. There is a small deviation between 160 and 190 K, which may arise from quantum phase slips. The fitting parameters are $m = (1.64\pm0.14)\times10^7$ kΩ$K^{1.5}$ and $c = 10.27\pm0.23$. It is striking that the values of $\beta$ and $c$ are also very close, similar to the case of the SWNT bundle with $T_{c0} = 0.44$ K.
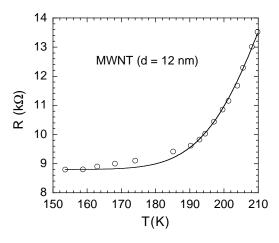


FIG. 6. The temperature dependence of the resistance for the 12-nm MWNT below about $0.15R_N$. The solid line is the curve best fitted by Eq. 7 with the fitting parameters: $m = (1.64\pm0.14)\times10^7$ kΩ$K^{1.5}$ and $c = 10.27\pm0.23$.

4

From the values of $m$, $c$, and $T_{c0}$, we can evaluate the zero-temperature coherence length $\xi(0)$ using Eq. 2. Substituting $m = 1.64 \times 10^7$ k$\Omega K^{1.5}$, $c = 10.27$, $T_{c0} = 262$ K, and $L = 5000$ Å into Eq. 2, we obtain $\xi(0) = 18.3$ Å. From the measured $R_N/L = 68$ k$\Omega/\mu$m and the relation $R_N/L = R_Q/N_{ch}l$ (Ref.[14]), we can calculate $N_{ch}l = 1897$ Å. Substituting $c = 10.27$ into Eq. 3, we get $N_{ch} = 30.2\xi_{BCS}/\xi(0)$. By solving the three equations: $N_{ch}l = 1897$ Å, $N_{ch} = 30.2\xi_{BCS}/\xi(0)$, and $\xi(0) = 0.74\xi_{BCS}\sqrt{\chi(0.882\xi_{BCS}/l)}$, we finally obtain $l = 35$ Å, $N_{ch} = 54$, and $\xi_{BCS} = 33.0$ Å. Here the Gorkov function $\chi(x)$ is defined as[7]

$$\chi(x) = \sum_{n=0}^{\infty} \frac{0.95}{(1+2n)^2(1+2n+x)}. \qquad (8)$$

The fact that $l \simeq \xi_{BCS}$ indicates that the LAMH theory (Eq. 7) is valid only below $0.17R_N$ (Ref.[7]). This justifies the region of the data we select to fit.

We can also evaluate the Fermi velocity $v_F$ from the deduced value of $\xi_{BCS}$ and the formula $\xi_{BCS} = 0.18\hbar v_F/k_B T_{c0}$. With $\xi_{BCS} = 33$ Å and $T_{c0} = 262$ K, we get $\hbar v_F = 4.14$ eVÅ. Using the value of $\gamma_\circ = 2.4$ eV estimated from the first principle calculation[11] and the relation $\hbar v_F = 1.5a_{C-C}\gamma_\circ$ (Ref.[10]) for the first subband of metallic chirality tubes, we obtain $\hbar v_F = 5.1$ eVÅ. It is remarkable that the value of $\hbar v_F$ deduced from the LAMH theory is about 20% lower than the value expected for the first subband of metallic chirality tubes. Such a small discrepancy may be explained by a fact that the Fermi level of some outer shells is crossing the second or higher subband where[15] the Fermi velocity is smaller than the one for the first subband. This quantitative agreement provides compelling evidence for high-temperature superconductivity at 262 K in this 12-nm MWNT.

Now we show that the deduced $N_{ch} = 54$ is also reasonable. For the MWNT with $d = 12$ nm, the total number of shells can be estimated to be about 17 using the fact that the intershell distance is 0.34 nm. This implies that the average number of the conducting channels per shell is about 3.2. This is possible when the Fermi level of some outer shells crosses their second subband (see above), which have 6 channels for a metallic chirality shell and 4 channels for a semiconducting chirality shell[10].

In fact, we can estimate the lower limit of the average number of conducting channels per shell for an 18-nm MWNT from the measured room-temperature four-probe resistance, which is 200 $\Omega$ (Ref.[12]). Using the relation $R = R_Q/tN_{ch} + R_{tube} \geq R_Q/N_{ch}$, and from $R = 200$ $\Omega$, we get $N_{ch} \geq 64$. The total number of shells for the 18-nm MWNT should be about 26. This implies that the average number of conducting channels per shell for the 18-nm MWNT is larger than 2.5, in agreement with that (3.2) deduced independently for the 12-nm MWNT.

One of the puzzling features of the resistive behavior for this 18-nm MWNT is the metal-insulator transition below about 200 K (Ref.[12]). We can attribute this to a superconductor-insulator transition in dirty quasi-1D systems. It is shown that when the thermal length is larger than the localization length below a temperature $T_{loc}$ in quasi-1D systems, the Anderson localization sets in and the ground state becomes insulating charge density wave (CDW)[16]. If we make a heterojunction between this insulating MWNT and other metal, we should expect a rectification effect below $T_{loc}$. The rectification effect will disappear above $T_{loc}$, in contrast to the conventional rectification effect which vanishes at a temperature far higher than $E_g/k_B$, where $E_g$ is the gap of a semiconductor. Kim et al. made a heterojunction between an insulating MWNT and a "conducting" MWNT[17]. The diameters of both tubes are 30 nm. The single-particle tunneling spectrum[17] indicates that $E_g$ for the insulating tube is about 150 meV. It is very unusual that[17] the rectification effect disappears above 192 K. This cannot be explained by the conventional model because 192 K is far below $E_g/k_B = 1740$ K. Furthermore, according to a formula $E_g = 2a_{C-C}\gamma_\circ/d$ (Ref.[10]), the predicted $E_g$ for a semiconducting chirality tube with $d = 30$ nm should be about 22 meV, which is about one order of magnitudes smaller than the observed gap for the insulating tube. On the other hand, the tunneling spectrum for another "conducting" tube[17] is consistent with $E_g \simeq 20$ meV, suggesting that the "conducting" tube has a semiconducting chirality. In order to consistently explain these novel behaviors, we must assume that the insulating tube has a metallic chirality and undergoes a transition from the superconducting to the insulating CDW ground state below $T_{loc} \simeq 192$ K. It is naturally expected that the observed metal-insulator transition below about 200 K in the 18-nm MWNT[12] should have the same origin as the 30-nm MWNT. Then, the half gap $E_g/2 \simeq 75$ meV for the insulating tube should be related to the minimum single-particle excitation gap in the CDW ground state. This also implies that the minimum superconducting gap would be about 75 meV if this 30-nm MWNT were clean enough to avoid the Anderson localization. The value of the superconducting gap suggests $T_{c0} > E_g/3.52k_B \simeq 500$ K, in agreement with the resistive transition in a MWNT mat (see below).

## V. THE RESISTIVE TRANSITION IN A SWNT MAT WITH $T_{C0} = 710$ K

Single-walled carbon nanotubes, prepared by metal-catalysed laser ablation of graphite, form closely-packed crystalline bundles. The bulk samples, or mats consist of entangled bundles that are contacted each other and oriented randomly[18]. If close-packed crystalline bundles are superconductors, the bulk samples should behave like granular superconductors. Depending on the Josephson coupling strength between the superconducting "grains", the ground state could be metallic, insulating, or superconducting[19]. It is interesting that the contact barrier resistance of a granular supercon-

ductor follows a rather unusual exponential temperature dependence in a certain temperature range[19], that is, $R_b(T) = R_b(0) \exp(BT)$, where $B$ could be positive, negative, or zero. This temperature dependence of the barrier resistance was also suggested[20] for the intertube barrier resistance in MWNTs. The barrier resistance extrapolated to zero temperature is finite even if the $T$-dependence of the resistance behaves like an insulator. This unique resistive behavior makes a clear distinction from that for conventional semiconductors where the resistance at zero temperature goes to infinity.

Fig. 7 shows the temperature dependence of the resistivity for a SWNT mat. The data are extracted from Ref.[18]. Below 200 K the resistivity is nearly temperature independent while above 200 K the resistivity increases suddenly and starts to flatten out above 550 K. This behavior is similar to that for a granular superconductor. Below we will show that this is indeed the case.
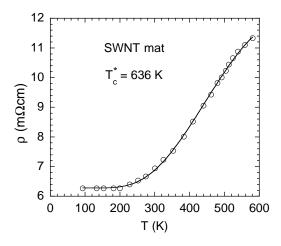


FIG. 7. The temperature dependence of the resistivity for a SWNT mat. The data are extracted from Ref.[18]. The solid line is the curve fitted by Eq. 9 with the fitting parameters: $\rho_0$= 6.277±0.018 mΩcm, $\beta$ = 0.90±0.04, and $T_c^*$ = 636.3 K.

We fit the resistivity data by

$$\rho = \rho_0(T) + \alpha \exp[-\frac{3\beta T_c^*}{T}(1 - \frac{T}{T_c^*})^{3/2}]. \quad (9)$$

Here the first term is the intertube contact barrier resistivity, which could be temperature dependent, and the second term is the on-tube resistivity that follows a simple exponential form same as Eq. 4. In the present case, the intertube barrier resistivity appears to be independent of temperature in the temperature region we are interested in, i.e., $B \simeq 0$. It is striking that the data can be well fitted by Eq. 9 with the fitting parameters: $\rho_0$= 6.277±0.018 mΩcm, $\beta$ = 0.90±0.04, and $T_c^*$ = 636.3 K. Using the relation $T_c^* = 0.895T_{c0}$ deduced empirically above, we obtain $T_{c0}$ = 710 K. It is remarkable that the $T_{c0}$ value obtained from the resistivity data is very close to that (665 K) inferred from the Raman data for a similarly prepared SWNT mat[1,2].

By extrapolation of the data shown in Fig. 7 to $T$ = 710 K, we estimate the normal-state on-tube resistivity at 710 K to be $\rho_N^{exp} \simeq 1.1\rho_N^{exp}(T_{c0})$= 6270 $\mu\Omega$cm. Since about one-third of tubes have metallic chiralities and the mat consists of crystalline bundles that are oriented randomly, the intrinsic normal-state on-tube resistivity $\rho_N^i$ of the superconducting tubes should be much smaller than $\rho_N^{exp}$= 6270 $\mu\Omega$cm, that is, $\rho_N^i = \rho_N^{exp}/f$, where $f$ is the reduction factor that should be close to 3(1/0.33) = 9. The intrinsic mean free path $l$ is related to $\rho_N^i$ by

$$l = \frac{R_Q}{2}\frac{A_\circ}{\rho_i}, \quad (10)$$

were $A_\circ$ is the area of single tube, which is equal to $1.54\times10^{-18}$ m$^2$ for $d$ =1.4 nm. If we take $f$ = 9, we get $l$ = 14 Å at T = 710 K from Eq. 10. If the resistivity jump above 200 K were due to inelastic scattering, the inelastic mean free path would be about 14 Å at about 700 K. This is inconsistent with any electrical transport mechanism for SWNTs.

Using $\hbar v_F$ = 4.5 eVÅ and $T_{c0}$ = 710 K, we find that the BCS coherence length along the tube-axis direction $\xi_{BCS}$ = 13.2 Å. The zero-temperature coherence length along the tube-axis direction $\xi(0)$ should be smaller than the clean-limit value: $0.74\xi_{BCS}$= 10 Å. Then the coherence length perpendicular to the tube axis should be order of 1 Å. Such a short coherence length implies that only those superconducting tubes that are adjacent to each other can have enough Josephson coupling to form a superconducting bundle. A simulation[21] indicates the average number of the metallic-chirality tubes that are adjacent to each other is about 2. This implies that the average number of the metallic-chirality tubes comprising a superconducting bundle is also about 2, and that there are a number of independent superconducting bundles within a physical bundle.

If we assume that the normal-state resistivity is linearly proportional to $T$ above 200 K, the average mean-free path between 200 K and 580 K should be about 26 Å, significantly larger than $\xi_{BCS}$. Then we estimate $\xi(0)$ $\simeq$ 8 Å. Using Eq. 3 and $c \simeq \beta$ = 0.9, we obtain $N_{ch} \simeq$ = 4.5. This implies that, on average, about two metallic chirality tubes are adjacent to each other and form a superconducting bundle, in quantitative agreement with the simulation[21].

## VI. THE RESISTIVE TRANSITION IN A MWNT MAT WITH $T_{C0}$ = 752 K

Multi-walled carbon nanotubes are prepared by arc discharge of graphite. A multi-walled carbon nanotube is packed in such a way that each shell is concentric with each other. If each shell has phase-incoherent superconductivity, MWNTs are almost optimally packed to maximize the Josephson coupling and phase coherence. Individual MWNTs can be closely packed into bundles. The

bulk samples, or mats are made of entangled bundles that are contacted each other and oriented randomly. The bulk samples should also behave like granular superconductors.

Fig. 8 shows the temperature dependence of the resistance for a MWNT mat. It is interesting that the resistance decreases monotonically with increasing temperature below about 570 K. Above 570 K, the resistance tends to turn up. The resistance between 300 K and 450 K can be excellently described by $17.3\exp(-T/618.3)$ Ω. This temperature dependence is expected for an intertube barrier resistance[20]. This implies that the on-tube resistance between 300 K and 450 K is negligible, in agreement with several independent experiments which consistently show a negligible on-tube resistance at room temperature in many individual MWNTs[22−25]. The observed finite and very small on-tube resistances in the individual MWNTs[24] are consistent with quasi-1D room-temperature superconductivity with finite quantum phase slips.
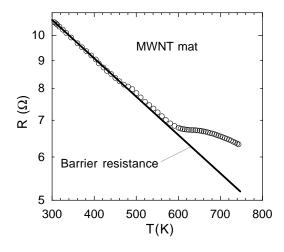


FIG. 8. The temperature dependence of the resistance for a MWNT mat. The data are the same as those in Ref.[27] but less data points are plotted for charity. The resistance between 300 K and 450 K can be excellently described by $17.3\exp(-T/618.3)$ Ω, which represents the intertube barrier resistance[20].

If we assume that this temperature dependence for the intertube barrier resistance remains valid up to 750 K, we then obtain the on-tube resistance by subtracting the barrier resistance from the total resistance. The resultant on-tube resistance below 665 K is shown in Fig. 9. The solid line is the fitted curve by Eq. 5 by excluding the data points between 450 K and 600 K. The shoulder feature between 450 K and 600 K may be caused by quantum phase slips or by bad electrical contacts. The fitting parameters are $\beta = 11.34$ and $T_c^* = 669$ K. Using the empirical relation $T_c^* = 0.89 T_{c0}$, we obtain $T_{c0} = 752$ K.
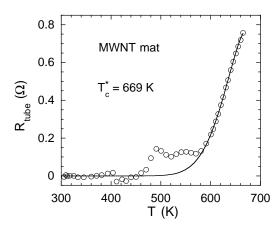


FIG. 9. The on-tube resistance by subtracting the barrier resistance from the total resistance of the MWNT mat. The solid line is the fitted curve by Eq. 5 by excluding the data points between 450 K and 600 K. The fitting parameters are $\beta = 11.34$ and $T_c^* = 669$ K.

It is interesting that the value of $\beta = 11.34$ for this MWNT mat is slightly smaller than that (11.71) for the 12-nm MWNT. This implies that, on average, the total number of transverse channels for each superconducting bundle (which may contain one or more MWNTs near $T_{c0}$) is comparable with that for the single 12-nm MWNT.
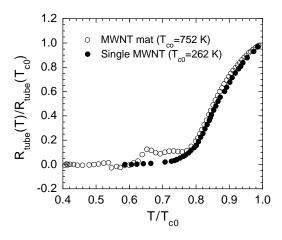


FIG. 10. The normalized on-tube resistance versus $T/T_{c0}$ for the 12-nm MWNT ($T_{c0} = 262$ K) and for the MWNT mat ($T_{c0} = 752$ K). The on-tube resistive transitions for the two systems are nearly identical although they have different $T_{c0}$'s.

In Fig. 10, we plot the normalized on-tube resistance versus $T/T_{c0}$ for the 12-nm MWNT ($T_{c0} = 262$ K) and for the MWNT mat ($T_{c0} = 752$ K). It is remarkable that the on-tube resistive transitions for the two systems are nearly identical although they have different $T_{c0}$'s and the electrical measurements were done by independent groups. This agreement also suggests that both data sets are reliable and that the procedure to extract the on-tube

resistance for the MWNT mat is justified.

## VII. MAGNETIC PROPERTIES OF MWNTS

From the quantitative analyses of the electrical transport data in several carbon nanotubes, we can clearly see that the superconducting transition temperatures can vary from 0.4 K to 750 K for different samples. We believe that the $T_{c0}$ variation may be associated with the differences in the doping level, the chirality and diameter of tubes, and in disorders. A similar $T_{c0}$ variation is seen in the graphite-sulfur system; $T_{c0}$ varies from 9 K to 250 K (Ref.[26]). In order to unambiguously show that high-temperature superconductivity in carbon nanotubes is real, one needs to provide magnetic evidence such as the Meissner effect. However, the Meissner effect may be less visible because the diameters of the tubes may be much smaller than the magnetic penetration depth. Further, the orbital diamagnetic susceptibility in the magnetic field perpendicular to the graphite sheet is large, making it difficult to separate the Meissner effect from the large orbital diamagnetic susceptibility. Fortunately, the orbital diamagnetic susceptibility of carbon nanotubes in the magnetic field parallel to the tube axis is predicted to be very small at room temperature[29]. This makes it possible to extract the Meissner effect from the measured susceptibility in the parallel field.
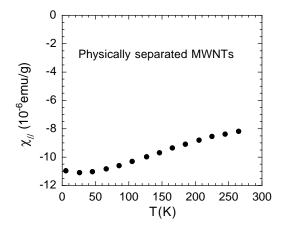
FIG. 11. The temperature dependence of the susceptibility for physically separated and aligned MWNTs in a magnetic field parallel to the tube axis. The data are extracted from Ref.[28].

Fig. 11 shows the temperature dependence of the susceptibility for physically separated and aligned MWNTs in a magnetic field parallel to the tube axis. The diameters of the tubes are 10±5 nm, and the lengths are on the order of 1 $\mu$m. It is apparent that the diamagnetic susceptibility is significant up to 265 K. Because the orbital diamagnetic susceptibility in the parallel field is negligible at room temperature[29], the observed diamagnetic susceptibility at 265 K should mainly contribute

from the Meissner effect due to superconductivity. Thus, the Meissner effect at 265 K is about -0.8×10$^{-5}$ emu/g, which is significant. This result clearly indicates that the superconducting transition temperature should be higher than 300 K.
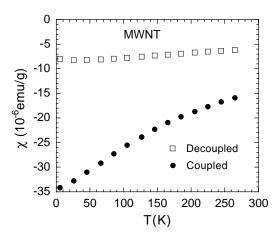
FIG. 12. The temperature dependence of the angle-averaged susceptibility for physically separated MWNTs (open squares) and for physically coupled MWNT mat (solid circles). The physically coupled mat sample is not processed so that the tubes are closely packed into bundles. The data are extracted from Ref.[28].

For superconducting tubes of radius $r$ in the magnetic field parallel to the tube axis, the diamagnetic susceptibility due to the Meissner effect is given by

$$\chi_\parallel^S(T) = -\frac{\bar{r^2}}{32\pi\lambda_\theta^2(T)}. \tag{11}$$

Here $\bar{r^2}$ is the average value of $r^2$, and $\lambda_\theta(T)$ is the penetration depth when carriers move along the circumferential direction. The above equation is valid only if $\lambda_\theta(0)$ is larger than the maximum radius of tubes, which should be the case for carbon nanotubes. Eq. 11 indicates that the Meissner effect is inversely proportional to $1/\lambda_\theta^2(T)$. Assuming an isotropic gap and taking $T_{c0} = 752$ K, we find that $1/\lambda_\theta^2(T)$ and thus $\chi_\parallel^S(T)$ are nearly independent of temperature below 265 K. Then we have $\chi_\parallel^S(0) =$ -0.8×10$^{-5}$ emu/g. If we assume that the radii of tubes are equally distributed from 0 to 100 Å, we find $\bar{r} = 50$ Å and $\bar{r^2}= 3333$ Å$^2$. With the weight density of 2.17 g/cm$^3$ (Ref.[30]) and $\chi_\parallel(0) = -0.8 \times 10^{-5}$ emu/g, we calculate $\lambda_\theta(0) \simeq 1380$ Å. The value of the penetration depth corresponds to $n/m_\theta^* = 1.48 \times 10^{21}$/cm$^3 m_e$, where $n$ is the carrier density, $m_\theta^*$ is the effective mass of carriers along the circumferential direction. If we take $m_\theta^* = 0.012\, m_e$, typical for graphites[31], we estimate $n = 1.78 \times 10^{19}$/cm$^3$, in good agreement with the Hall effect measurement[20] which gives $n = 1.6 \times 10^{19}$/cm$^3$. It is worthy of noting that the Hall coefficient in the physically separated MWNTs does not go to zero below $T_{c0}$. This

is because the on-tube resistance does not exactly go to zero due to quantum phase slips and because the magnetic field is almost penetrated into the whole volume of the tubes.

From Eq. 11, we can see that $\chi_{\parallel}^{S}(T)$ will increase linearly with increasing $\bar{r^2}$ or cross-sectional area. For Josephson coupled MWNT bundles in unprocessed mats, the effective $\bar{r^2}$ is larger than that for physically separated tubes. As the temperature decreases, the Josephson coupling strength increases so that the effective $\bar{r^2}$ and $\chi_{\parallel}^{S}(T)$ also increases. This can naturally explain why the diamagnetic susceptibility for physically coupled MWNTs is larger than that for physically separated MWNTs and why the enhancement in the diamagnetic susceptibility increases significantly with decreasing temperature (see Fig. 12). At the lowest temperature, the enhancement factor is about 4.3. Without superconductivity in these MWNTs, it is very difficult to account for such a large enhancement in the diamagnetic susceptibility upon bundling of the tubes.

## VIII. CONCLUSION

In summary, we have made quantitative data analyses on the observed resistive transitions and magnetic properties in carbon nanotubes. We show that the resistive transitions in various carbon nanotube samples with $T_{c0}$ varying from 0.4 K to 750 K all agree with the theoretical predictions for quasi-1D superconductors in a quantitative way. We have also identified the Meissner effect in the field parallel to the tube axis up to room temperature for aligned MWNTs that are physically separated. The magnitude of the Meissner effect is in quantitative agreement with the predicted penetration depth from the measured carrier density. Furthermore, the diamagnetic susceptibility in closely packed MWNT bundles increases by a factor of over 4 at low temperatures compared with that for physically separated tubes. This is the hallmark of the Josephson coupling among the tubes in bundles. These results consistently indicate quasi-1D high-temperature superconductivity in carbon nanotubes.

Correspondence should be addressed to gzhao2@calstatela.edu.

[1] G. M. Zhao, cond-mat/0307770.

[2] G. M. Zhao, Molecular Nanowires and Other Quantum Objects edited by A. S. Alexandrov, J. Demsar and I. K. Yanson (Nato Science Series, Kluwer Academic Publishers, Netherlands, 2004) page 95-106.

[3] J. S. Langer and V. Ambegaokar, Phys. Rev. **164**, 498 (1967); D. E. McCumber and B. I. Halperin, Phys. Rev. B **1**, 1054 (1970).

[4] A. D. Zaikin, D. S. Golubev, A. van Otterlo, and G. T. Zimanyi, Phys. Rev. Lett. **78**, 1552 (1997).

[5] G. M. Zhao, cond-mat/0409216.

[6] C. Schönenberger, A. Bachtold, C. Strunk, J.-P. Salvetat, L. Forro, Appl. Phys. A **69**, 283 (1999).

[7] J. R. Trucker and B. I. Halperin, Phys. Rev. B **3**, 3768 (1971).

[8] M. Kociak, A.Yu. Kasumov, S. Gueron, B. Reulet, I. I. Khodos, Yu. B. Gorbatov, V. T. Volkov, L. Vaccarini, and H. Bouchiat, Phys. Rev. Lett. **86**, 2416 (2001).

[9] G. M. Zhao, cond-mat/0208198.

[10] J. W. Mintmire and C. T. White, Phys. Rev. Lett. **81**, 2506 (1998).

[11] J. W. Mintmire, B. I. Dunlap, and C. T. White, Phys. Rev. Lett. **68**, 631 (1992).

[12] T. W. Ebbesen, H. J. Lezec, H. Hiura, J. W. Bennett, H. F. Ghaemi, and T. Thio, Nature (London) **382**, 54 (1996).

[13] Private communications with Prof. T. W. Ebbesen.

[14] L. X. Bendedict, V. H. Crespi, S. G. Louie, and M. L. Cohen, Phys. Rev. B **52**, 14935 (1995).

[15] R. Saito, M. Fujita, G. Dresselhaus, and M. S. Dresselhaus, Phys. Rev. B **46**, 1804 (1992).

[16] E. Orignac and T. Giamarchi, Phys. Rev. B **56**, 7167 (1997).

[17] Jinhee Kim, Jeong-O Lee, Hwangyou Oh, Kyung-Hwa Yoo, and Ju-Jin Kim, Phys. Rev. B **64**, 161404R (2001).

[18] R. S. Lee, H. J. Kim, J. E. Fischer, A. Thess, and R. E. Smalley, Nature (London) **388**, 255 (1997).

[19] L. Merchant, J. Ostrick, R. P. Barber, Jr., and R. C. Dynes, Phys. Rev. B **63**, 134508 (2001).

[20] G. Baumgartner, M. Carrard, L. Zuppiroli, W. Bacsa, Walt A. de Heer, and L. Forro, Phys. Rev. B **55**, 6704 (1997).

[21] H. Stahl, J. Appenzeller, R. Martel, Ph. Avouris, and B. Lengeler, Phys. Rev. Lett. **85**, 5186 (2000).

[22] S. Frank et al., Science **280**, 1744 (1998).

[23] P. J. de Pablo, E. Graugnard, B. Walsh, R. P. Andres, S. Datta, and R. Reifenbergera, Appl. Phys. Lett. **74**, 323 (1999).

[24] P. Poncharal, C. Berger, Y. Yi, Z. L. Wang, W. A. de Heer, J. Phys. Chem. B 106, 12104 (2002).

[25] A. Urbina, I. Echeverra, A. Perez-Garrido, A. Daz-Sanchez, and J. Abellan, Phys. Rev. Lett. **90**, 106603 (2003).

[26] Y. Kopelevich, R. R. da Silva, J. H. S. Torres, S. Moehlecke, and M. B. Maple, preprint.

[27] G. M. Zhao and Y. S. Wang, cond-mat/0111268.

[28] O. Chauvet, L. Forro, W. Bacsa, D. Ugarte, B. Doudin, and W. A. de Heer, Phys. Rev. B **52**, R6963 (1995). The aligned nanotube films were produced by a process in which the tubes are ultrasonically separated.

[29] J. P. Lu, Phys. Rev. Lett. **74**, 1153 (1995).

[30] D. Qian et al., Appl. Phys. Lett. **76**, 2828 (2000).

[31] V. Bayot et al., Phys. Rev. B **40**, 3514 (1989).